

## Toward highly efficient photocatalysis: a flow-through $\text{Pt@TiO}_2@\text{AAO}$ membrane nanoreactor prepared by atomic layer deposition†

Hsueh-Shih Chen,\* Po-Hsun Chen, Sheng-Hsin Huang and Tsong-Pyng Perng\*

Cite this: *Chem. Commun.*, 2014, 50, 4379

Received 13th February 2014,  
Accepted 7th March 2014

DOI: 10.1039/c4cc01166j

[www.rsc.org/chemcomm](http://www.rsc.org/chemcomm)

**A  $\text{Pt@TiO}_2@\text{AAO}$  membrane nanoreactor was fabricated by atomic layer deposition. The photodegradation test of methylene blue demonstrated that the nanoreactor shows efficient photocatalysis performance. It exhibited  $\sim 28\%$  photodegradation of methylene blue after ten flow-through cycles, corresponding to about  $2.7 \times 10^{-2}$  s of contact time of methylene blue with  $\text{Pt@TiO}_2$  nanotubes.**

Reactions taking place in a nanovessel are of great interest. In a nanospace, molecular reactions could be selectively and/or spatially confined so the reaction kinetics/thermodynamics might be different from those in a macrosystem.<sup>1</sup> In order to explore this novel field, fabrication of nanovessels or nanoreactors has attracted much attention recently.<sup>2</sup> Nanovessels used as reactors, *i.e.*, nanoreactors, can be cataloged into batch-type and continuous flow-type. More specifically, the batch-type nanoreactor, which usually makes use of nanostructured materials dispersed in a reaction mixture, allows reactants to be encapsulated or to permeate into the nanoreactor for reaction. It offers advantages of improved reaction selectivity and catalyst reactivity in an enclosed environment.<sup>3</sup> For example, hollow or yolk-shell nanocrystals that provide the shell for selective entry and the space between the core and shell for reaction were synthesized and proposed as a nanoreactor for catalysis.<sup>4</sup> Catalysts with such a hollow sphere encapsulation were also found to exhibit better thermal stability.<sup>5</sup> However, entry of reactants through the solid shell of the yolk-shell nanocrystals is limited. Therefore, alternative Pt/mesoporous silica core–shell nanocrystals, which offer more facile diffusion and transport of the reactants/products through the silica mesoporous shell, have also been reported.<sup>6</sup> On the other hand, a continuous flow nanoreactor may be realized by making use of porous materials or flow-through membranes such as mesoporous carbon, anodic aluminum oxide (AAO), or a polymer membrane coated with specific functional materials.<sup>7</sup> In general, continuous flow-type reactors provide more efficient heat transfer than batch ones. Moreover, the

space effect in a continuous flow nanoreactor could be predominant. For example, collisions between the reactant and nanoreactor wall can be enhanced when the dimensions of the nanoreactor decrease. Furthermore, in a very confined space, molecules might be deformed and their configuration could change. In that situation, reaction kinetics and thermodynamic equilibrium might be very different from those in a macrosystem.

Atomic layer deposition (ALD) has been widely employed to coat functional metal oxides on different templates.<sup>8</sup> It offers advantages such as an atomically smooth surface, precise control of the film thickness on the atomic scale, conformality, and scale-up capability. By using a suitable template, ALD is considered as one of the best techniques to prepare nanovessels for nanoreactions. In this communication, we demonstrate a flow-through  $\text{Pt@TiO}_2$  membrane nanoreactor prepared by ALD using AAO as a support, *i.e.*, the  $\text{Pt@TiO}_2@\text{AAO}$  membrane nanoreactor. Pt nanoparticles (NPs) with a size of 1–5 nm were grown on the  $\text{TiO}_2$  nanotube inner wall. The  $\text{Pt@TiO}_2@\text{AAO}$  membrane nanoreactor showed promising performance for photocatalytic reactions.

$\text{TiO}_2$  nanotubes or nanotube arrays have been considered as active catalysts for photocatalytic reactions. However, photocatalytic reactions generally take place outside the nanotubes if the diameter of nanotubes is too small because surface tension, viscosity, and size/shape would limit the entry of reactants into the nanotubes. Therefore, the nanotubes only provide a larger outer surface area or more reactive sites for reaction. In the present design of a flow-through membrane reactor, AAO is used as a support which allows reactants to flow through the membrane pores. By coating the catalyst on the inner wall of AAO nanopores, the reactants would interact with the catalyst in a nanospace when they flow through the nanopores.

The ALD technique and apparatus have been reported previously.<sup>9</sup> Deposition of  $\text{TiO}_2$  was carried out by horizontal flow-type ALD, in which  $\text{TiCl}_4$  and  $\text{H}_2\text{O}$  were used as precursors.<sup>10</sup> The substrate temperature was 100 °C and working pressure was 2 mTorr. The purge times of  $\text{TiCl}_4$  and  $\text{H}_2\text{O}$  were 0.4 s and 0.2 s, respectively, and 5 s  $\text{N}_2$  gas purge was used to separate all precursor pulses. The growth-per-cycle (GPC) of  $\text{TiO}_2$  was approximately 0.58 Å per cycle.  $\text{TiO}_2@\text{AAO}$  membrane nanoreactors

Department of Materials Science and Engineering, National Tsing Hua University, Hsinchu 300, Taiwan. E-mail: [chenhs@mx.nthu.edu.tw](mailto:chenhs@mx.nthu.edu.tw), [tpperng@mx.nthu.edu.tw](mailto:tpperng@mx.nthu.edu.tw)

† Electronic supplementary information (ESI) available. See DOI: 10.1039/c4cc01166j

were prepared by ALD using the commercial open through-pore AAO membrane (Whatman Anodisc, dia. = 13 mm, thickness = 50  $\mu\text{m}$ ) as a template. The actual pore diameter was approximately 145 nm. The ALD of  $\text{TiO}_2$  was performed first to form a  $\text{TiO}_2@\text{AAO}$  structure.<sup>10b,c</sup>

After deposition of  $\text{TiO}_2$  onto the AAO template, the  $\text{TiO}_2$  overlayer on the template was removed by mechanical polishing with colloidal  $\text{SiO}_2$  solution. Pt NPs were then deposited on  $\text{TiO}_2$  by vertical flow-type ALD to produce a  $\text{Pt}@\text{TiO}_2@\text{AAO}$  composite structure.  $\text{MeCpPtMe}_3$  and oxygen were used as precursors for deposition of Pt.<sup>11</sup> In each cycle,  $\text{MeCpPtMe}_3$  pulse (1 s) and  $\text{O}_2$  pulse (5 s) were separated by 20 s of  $\text{N}_2$  purge. The Pt deposition was carried out for 50 cycles at 350 °C. The as-prepared  $\text{TiO}_2@\text{AAO}$  and  $\text{Pt}@\text{TiO}_2@\text{AAO}$  membrane nanoreactors were annealed at 450 °C for 2 h to assure conversion of  $\text{TiO}_2$  to the anatase phase. For TEM characterization of  $\text{Pt}@\text{TiO}_2$ , AAO was removed by immersing the sample in NaOH solution. To study the photocatalysis performance of the nanoreactors, methylene blue ( $\text{C}_{16}\text{H}_{18}\text{N}_3\text{SCl}$ , MB) was used as a test reagent. 30 ml of  $2 \times 10^{-6}$  M MB aqueous solution was loaded into the nanoreactor system and placed in the dark for 20 min. The solution was then repeatedly circulated through the nanoreactor using a dry pump. Each flow-through cycle is defined as a complete process of MB solution flowing through the membrane nanoreactor with the average flow rate of  $\sim 0.06 \text{ ml s}^{-1}$  for 30 ml of MB. The reaction temperature was kept at 24 °C. A black-light UV-A lamp equipped with a filter (Blak-Ray B-100,  $\lambda = 365 \text{ nm}$ ) was used as the light source. A blank experiment in the dark was conducted for reference. The variation of MB concentration was measured by UV-vis spectroscopy.

Fig. 1 shows the schematic ALD processes of fabricating  $\text{TiO}_2$  and  $\text{Pt}@\text{TiO}_2$  membrane nanoreactors using AAO as a template and support. AAO is first coated with  $\text{TiO}_2$  thin film to form AAO-supported  $\text{TiO}_2$  nanochannels, followed by depositing Pt NPs on the inner wall of  $\text{TiO}_2$ . Each Pt-loaded  $\text{TiO}_2$  tube acts as a tubular reactor that provides a nano-spaced channel. A piece of the AAO membrane with a diameter of 13 mm generally contains more than  $10^9$  pores with the average pore diameter of  $\sim 145 \text{ nm}$ , so a

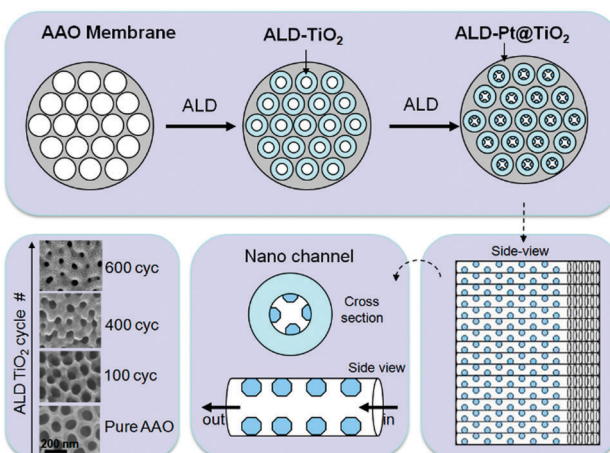


Fig. 1 Fabrication of flow-through membrane nanoreactors using AAO as a template and support.  $\text{TiO}_2$  is coated onto the pores of AAO by ALD. Pt NPs are then directly deposited on the inner wall of  $\text{TiO}_2$  by ALD. The diameter of  $\text{TiO}_2$  nanochannels is controlled by the ALD cycle number for  $\text{TiO}_2$  (lower left).

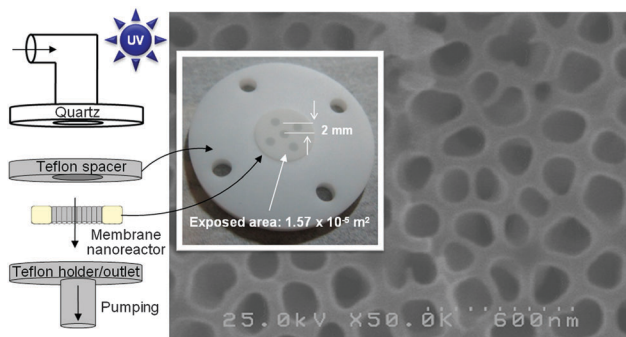


Fig. 2 Design of the flow-through membrane nanoreactor system (left illustration). The nanoreactor is sandwiched in two Teflon plates. The membrane is wrapped with a plastic tape along the edge and fixed by the Teflon holder which also acts as the outlet connected to a dry pump. The right SEM image shows the top view of the nanoreactor membrane. The inset photo shows the membrane nanoreactor together with the Teflon spacer possessing five holes allowing UV light illumination of the nanoreactor.

membrane nanoreactor provides a large number of nanochannels for reaction. The inner diameter of  $\text{TiO}_2$  tubes could be controlled by the thickness of  $\text{TiO}_2$  coating or the number of the ALD cycle, as shown by the SEM images (lower left) in Fig. 1. As the number of the ALD cycle increases, the inner diameter of  $\text{TiO}_2$  tubes decreases. Fig. 2 (left sketch) shows the design of a photocatalytic reaction system using the  $\text{TiO}_2@\text{AAO}$  or  $\text{Pt}@\text{TiO}_2@\text{AAO}$  membrane as a nanoreactor. The quartz window allows solar or UV light to illuminate the membrane nanoreactor. A spacer made of Teflon with five holes (dia. = 2 mm), loaded between the membrane nanoreactor and the quartz window, is used to fix the membrane and control the illuminated area. For 400-cycle  $\text{TiO}_2$  on AAO ( $\text{TiO}_2$  thickness  $\sim 22 \text{ nm}$ ), the inner diameter of the  $\text{TiO}_2$  tube is approximately 101 nm. A  $\text{TiO}_2@\text{AAO}$  membrane provides approximately  $4.08 \times 10^8$  tubes in the illuminated area. Therefore, total tube volume in the illuminated region is approximately  $1.63 \times 10^{-4} \text{ ml}$ .

Fig. 3a shows a representative transmission electron microscopic (TEM) image of a  $\text{TiO}_2$  tube (400 cycles of ALD) deposited with Pt NPs (50 cycles of ALD) from a  $\text{Pt}@\text{TiO}_2@\text{AAO}$  membrane nanoreactor after removing AAO. The inset shows a lower magnification image. The  $\text{TiO}_2$  tube contains numerous Pt NPs with the diameter of 1–5 nm on the surface of the inner wall. Pt grown by ALD with a few cycles normally forms small nanoparticles before continuous Pt film forms when (*methylcyclopentadienyl*)trimethylplatinum ( $\text{MeCpPtMe}_3$ ) and  $\text{O}_2$  are employed as precursors.<sup>12</sup> A TEM image of  $\text{Pt}@\text{TiO}_2$  annealed at 450 °C for 2 h is shown in Fig. 3b. Note that the Pt NPs are deposited on the inner wall of the  $\text{TiO}_2$  tube so images of the Pt NPs are slightly blurred. A high-resolution TEM image of a Pt NP on  $\text{TiO}_2$  is shown in Fig. 3c. The lattice fringes indicate that both Pt and  $\text{TiO}_2$  have good crystallinity. The interplanar spacings of Pt NP and  $\text{TiO}_2$  at the Pt– $\text{TiO}_2$  interface are measured to be 0.183 nm and 0.364 nm, respectively. In Fig. 3d, fast Fourier transform (FFT) analysis of the selected areas for  $\text{Pt}@\text{TiO}_2$  (yellow dashed lines, region 1), Pt NP (region 2), and  $\text{TiO}_2$  (region 3) shows the existence of Pt and  $\text{TiO}_2$  crystal lattices, indexed by  $\text{Pt}(200)$  and  $\text{TiO}_2(101)$ . The  $d$ -spacing of cubic Pt(200) is 0.196 nm (JCPDS-ICCD, #04-0802) and that of anatase  $\text{TiO}_2(101)$  is 0.352 nm

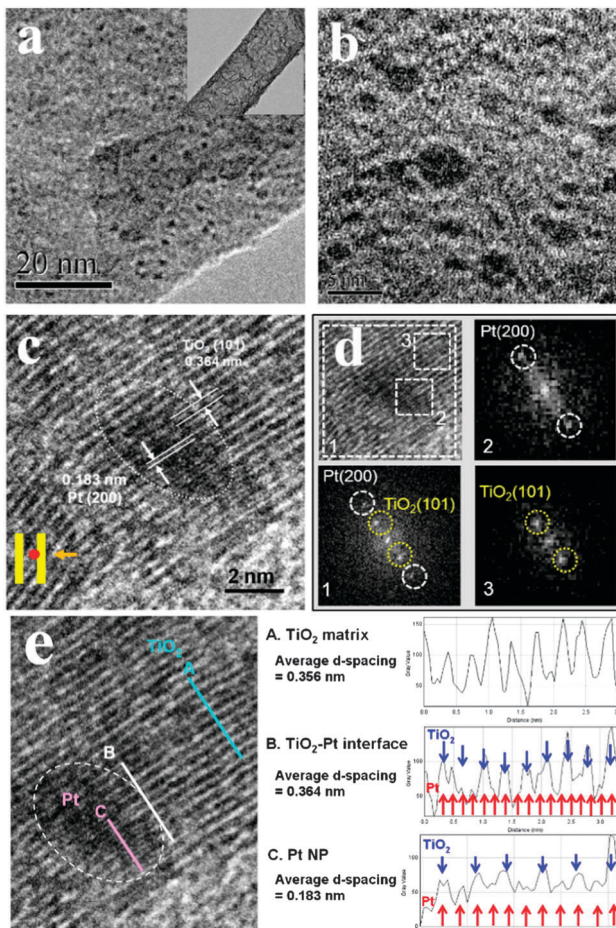


Fig. 3 TEM images of a Pt (50 cycles)@TiO<sub>2</sub> (400 cycles) nanotube. The AAO support was removed by NaOH aqueous solution. (a) A TiO<sub>2</sub> nanotube deposited with Pt NPs at 350 °C by ALD. The inset shows a low magnification image. (b) Pt@TiO<sub>2</sub> annealed at 450 °C for 2 h. Note that the Pt NP is located on the inner wall of TiO<sub>2</sub> nanotubes. (c) Lattice fringes of a selected annealed Pt@TiO<sub>2</sub> nanotube. (d) FFT analysis of different areas of the Pt@TiO<sub>2</sub> nanotube, and (e) profiles of lattice fringes of TiO<sub>2</sub> (line A), the TiO<sub>2</sub>-Pt interface (line B), and Pt NP (line C).

(JCPDS-ICCD, #21-1272). Therefore, the fringes in Fig. 3c could be assigned to the planes of Pt(200) and TiO<sub>2</sub>(101), respectively. The Pt(200) is interlaced with TiO<sub>2</sub>(101) and has approximately one half of the (101) spacing. Thus, the Pt lattice is compressed by ~6.6%, while the TiO<sub>2</sub> lattice is expanded by ~3.4%. The profiles of the lattice fringes of TiO<sub>2</sub>, the TiO<sub>2</sub>-Pt interface, and Pt NP are displayed in Fig. 3e. The above results suggest that Pt NPs have grown on the anatase TiO<sub>2</sub>(101) by the ALD process along with a post-heat treatment and that they possess good adhesion to the TiO<sub>2</sub> surface. The growth of Pt NPs or clusters on the anatase TiO<sub>2</sub>,<sup>13</sup> the Pt precursor has a higher probability to react with this surface. The loading of Pt NPs calculated from TEM images is approximately 1.7 µg cm<sup>-2</sup>.

In the nanoreactor, the average flow rate of MB solution was ~0.06 ml s<sup>-1</sup>. Since the length and inner diameter of a TiO<sub>2</sub> nanotube are ~50 µm and ~101 nm, respectively, the volume inside a TiO<sub>2</sub> nanotube is calculated to be 4.0 × 10<sup>-13</sup> cm<sup>3</sup>. The area

of the nanoreactor exposed to UV light is estimated to be ~1.57 × 10<sup>-5</sup> m<sup>2</sup>, which contains ~4.08 × 10<sup>8</sup> nanotubes with a total volume of 1.63 × 10<sup>-4</sup> cm<sup>3</sup>. Thus, the actual traveling time of MB molecules through the TiO<sub>2</sub> nanochannels in the nanoreactor is estimated to be ~2.7 × 10<sup>-3</sup> s in each cycle. For the annealed TiO<sub>2</sub>@AAO membrane nanoreactor, the photodegradation efficiency is significantly improved because of the higher photocatalytic performance of anatase TiO<sub>2</sub>. The Schottky barrier could reduce the electron-hole recombination and enhance electron-hole separation, thus enhancing the photocatalysis.<sup>15</sup>

It was noted from the dark test that some MB molecules were adsorbed on the TiO<sub>2</sub> membrane. A similar result was reported in a recent study, where a TiO<sub>2</sub>-coated AAO membrane filter was demonstrated to efficiently adsorb toluene molecules.<sup>7</sup> In the present study, this phenomenon gradually reduced the flow rate of MB aqueous solution through the membrane nanoreactor in the dark test. In order to eliminate the effect of adsorption of MB on the nanoreactor, the photodegradation curves are calibrated by using the dark reference curve as the baseline, as shown in the inset of Fig. 4. After the calibration, the photodecomposition of MB in the unannealed TiO<sub>2</sub>@AAO nanoreactor displays a small level-off decay against the cycle number. The annealed TiO<sub>2</sub>@AAO and Pt@TiO<sub>2</sub>@AAO nanoreactor curves, on the other hand, exhibit continuous decays. The overall decays after ten cycles are 3.2%, 20.3%, and 27.7% for as-prepared TiO<sub>2</sub>@AAO, annealed TiO<sub>2</sub>@AAO, and annealed Pt@TiO<sub>2</sub>@AAO nanoreactors, respectively, which mean that more than 1/4 MB can be photodegraded in about 2.7 × 10<sup>-2</sup> s (actual contact time with TiO<sub>2</sub> in ten cycles) by the annealed Pt@TiO<sub>2</sub>@AAO nanoreactor. Note that the illuminated region of the membrane nanoreactor is only 1.57 × 10<sup>-5</sup> m<sup>2</sup> in this case. The high photodegradation rate of MB could be ascribed to the space confinement effect that improves the mass transfer of MB to the TiO<sub>2</sub> surface in the nanoreactor which is to be discussed later.

In general, the photochemical reaction of organic molecules occurs on the nanosecond time scale,<sup>16</sup> while adsorption of MB onto

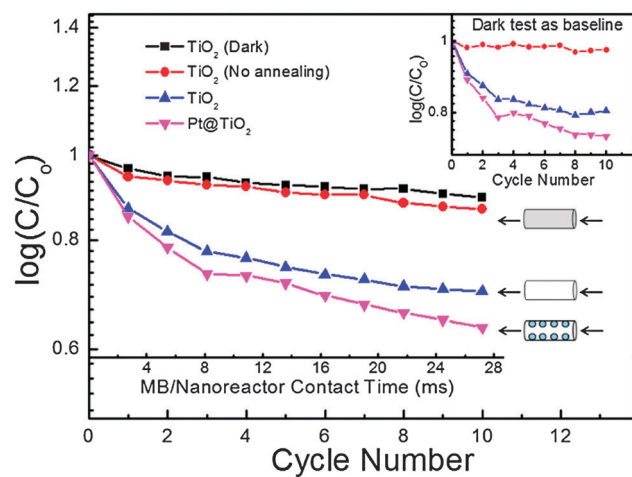


Fig. 4 Photodegradation of methylene blue by TiO<sub>2</sub>@AAO and Pt@TiO<sub>2</sub>@AAO membrane nanoreactors. A dark reference test of a TiO<sub>2</sub>@AAO nanoreactor (annealed) is given for comparison. The average flow rate of MB solution through the membrane nanoreactor is ~0.06 ml s<sup>-1</sup> for 30 ml of MB. The inset shows calibrated curves with the dark test as a baseline.

the  $\text{TiO}_2$  surface normally occurs on the minute scale depending on the concentration.<sup>17</sup> Therefore, the rate of MB photodecomposition is limited by the molecular diffusion or mass transfer to the photocatalyst surface and the degradation of MB generally takes hours in a  $\text{TiO}_2$  slurry. Since the continuous flow in the nanoreactor system improves the mass transfer of MB molecules, a higher performance of photodegradation is expected. However, the results may not be directly compared with that of the  $\text{TiO}_2$  slurry or batch-type nanoreactor, as the catalyst form, mass transfer, reaction system design, *etc.*, are different. A similar system design reported in the literature is a diffusion-based self-organized  $\text{TiO}_2$  nanotube membrane reactor (tube length  $\sim 145$   $\mu\text{m}$ , inner diameter  $\sim 140$  nm) in which no continuous flow was operated and the reactants migrated through the inside of pores and/or between the  $\text{TiO}_2$  nanotubes by diffusion.<sup>18</sup> In that study, it was reported that MB was oxidized on the illuminated surface of the membrane and completely disappeared by only one flow-through cycle, though the flow-through experimental time was 20 h due to a relatively low rate of diffusion.

In a general photocatalytic reaction with  $\text{TiO}_2$  powder slurry (bulk reaction), reactants and  $\text{TiO}_2$  particles are mixed in a bulk solution and thus the reaction kinetics is determined by the probability of molecular collisions, the surface area of the catalyst, product accumulation, *etc.* If  $\text{TiO}_2$  is a nanotube slurry, a small amount of reactant might migrate into the inside of the nanotube to carry out photocatalytic reactions. However, a larger part of the reaction still takes place on the outer surface of the nanotubes. For  $\text{TiO}_2$  nanotubes in the form of a membrane in the present case, the reactants can flow through the  $\text{TiO}_2$  nanotubes when a pressure drop is present between both sides of the membrane. Regarding the effect of nanosized channels in the membrane, two phenomena, *i.e.*, improved mass transfer and limited space to accommodate MB molecules, may be considered during the photocatalytic reaction. For the first phenomenon, MB solution is enforced to enter the nanochannels so there are relatively more MB molecules travelling over the  $\text{TiO}_2$  or  $\text{Pt@TiO}_2$  surface per unit time compared with that in a static solution. For the second effect, the nanospace confinement, the nanosized channels should not change the configuration of MB molecules since the channel diameter ( $\sim 100$  nm) is much larger than the MB molecular size ( $<2$  nm).<sup>19</sup> However, the motion of the flowing MB molecules may be significantly confined by the nanochannels. The diffusion length of MB is about 100  $\mu\text{m}$ ,<sup>20</sup> which is much larger than the diameter of  $\text{TiO}_2$  nanotubes, so collision of MB molecules with the  $\text{TiO}_2$  or  $\text{Pt@TiO}_2$  wall is increased within the nanochannels, known as Knudsen diffusion.<sup>21</sup> Moreover, the flow through-type nanoreactor works continuously, which avoids accumulation of products and by-products in the system to slow down the forward reaction.<sup>22</sup> Consequently, improved mass transfer, Knudsen diffusion caused by the nanospace confinement, and improved forward reaction enhance the photocatalysis of MB in the present membrane nanoreactor. In a practical application, more membrane nanoreactors can be assembled in series so that the actual contact time of each cycle can be extended and the efficiency can be further increased.

In summary,  $\text{TiO}_2@\text{AAO}$  and  $\text{Pt@TiO}_2@\text{AAO}$  flow-through membrane nanoreactors were fabricated by atomic layer deposition using AAO as a template. Pt nanoparticles with a diameter between 1 and 5 nm were grown on the inner wall of

$\text{TiO}_2$  nanotubes. It was observed that the overall decay of methylene blue in the  $\text{Pt@TiO}_2@\text{AAO}$  nanoreactor system was about 27.7% after ten flow-through cycles, equivalent to  $2.7 \times 10^{-2}$  s actual contact time on the catalyst in the  $1.57 \times 10^{-5}$   $\text{m}^2$  illuminated region. This study demonstrated that this membrane nanoreactor has promising applications in photocatalytic reactions.

This work was supported by the National Science Council of Taiwan under Contract no. NSC 99-2221-E-007-066-MY3 and NSC 101-2120-M-007-013.

## Notes and references

- 1 M. Polak and L. Rubinovich, *Nano Lett.*, 2008, **8**, 3543.
- 2 (a) D. H. Leung, D. Fiedler, R. G. Bergman and K. N. Raymond, *Angew. Chem., Int. Ed.*, 2004, **43**, 963; (b) Ch. Deneke, N. Y. Jin-Phillipp, I. Loa and O. G. Schmidt, *Appl. Phys. Lett.*, 2004, **84**, 4475; (c) C. W. Yen, M. A. Mahmoud and M. A. El-Sayed, *J. Phys. Chem. A*, 2009, **113**, 4340; (d) M. J. Monteiro, *Macromolecules*, 2010, **43**, 1159; (e) M. A. Mahmoud and M. A. El-Sayed, *Nano Lett.*, 2011, **11**, 946.
- 3 (a) D. M. Vriezema, M. C. Aragones, J. A. A. W. Elemans, J. J. L. M. Cornelissen, A. E. Rowan and R. J. M. Nolte, *Chem. Rev.*, 2005, **105**, 1445; (b) P. Cotanda, A. Lu, J. P. Patterson, N. Petzeltakis and R. K. O'Reilly, *Macromolecules*, 2012, **45**, 2377.
- 4 (a) Y. Yin, R. M. Rioux, C. K. Erdonmez, S. Hughes, G. A. Somorjai and A. P. Alivisatos, *Science*, 2004, **304**, 711; (b) Y. Yang, X. Liu, X. Li, J. Zhao, S. Bai, J. Liu and Q. Yang, *Angew. Chem., Int. Ed.*, 2012, **51**, 1.
- 5 (a) P. M. Arnal, M. Comotti and F. Schuth, *Angew. Chem., Int. Ed.*, 2006, **45**, 8224; (b) J. C. Park, J. U. Bang, J. Lee, C. H. Ko and H. Song, *J. Mater. Chem.*, 2010, **20**, 1239.
- 6 S. H. Joo, J. Y. Park, C. K. Tsung, Y. Yamada, P. Yang and G. A. Somorjai, *Nat. Mater.*, 2009, **8**, 126.
- 7 H. J. Lee, H. O. Seo, D. W. Kim, K. D. Kim, Y. Luo, D. C. Lim, H. Ju, J. W. Kim, J. Lee and Y. D. Kim, *Chem. Commun.*, 2011, **47**, 5605.
- 8 J. T. Korhonen, P. Hiekkataipale, J. Malm, M. Karppinen, O. Ikkala and R. H. A. Ras, *ACS Nano*, 2011, **5**, 1967.
- 9 C. C. Wang, C. C. Kei, Y. W. Yu and T. P. Perng, *Nano Lett.*, 2007, **7**, 1566.
- 10 (a) C. C. Wang, C. C. Kei and T. P. Perng, *Nanotechnology*, 2011, **22**, 365702; (b) Y. C. Liang, C. C. Wang, C. C. Kei, Y. C. Hsueh, W. H. Cho and T. P. Perng, *J. Phys. Chem. C*, 2011, **115**, 9498; (c) W. T. Chang, Y. C. Hsueh, S. H. Huang, K. I. Liu, C. C. Kei and T. P. Perng, *J. Mater. Chem. A*, 2013, **1**, 1987.
- 11 (a) Y. C. Hsueh, C. C. Wang, C. C. Kei, Y. H. Lin, C. Liu and T. P. Perng, *J. Catal.*, 2012, **294**, 63; (b) C. Liu, C. C. Wang, C. C. Kei, Y. C. Hsueh and T. P. Perng, *Small*, 2009, **5**, 1535; (c) T. Aaltonen, M. Ritala, T. Sajavaara, J. Keinonen and M. Leskela, *Chem. Mater.*, 2003, **15**, 1924.
- 12 (a) W. Setthapun, W. D. Williams, S. M. Kim, H. Feng, J. W. Elam, F. A. Rabuffetti, K. R. Poepelmeier, P. C. Stair, E. A. Stach, F. H. Ribeiro, J. T. Miller and C. L. Marshall, *J. Phys. Chem. C*, 2010, **114**, 9758; (b) L. Baker, A. S. Cavanagh, D. Seghete, S. M. George, A. J. M. Mackus, W. M. M. Kessels, Z. Y. Liu and F. T. Wagner, *J. Appl. Phys.*, 2011, **109**, 084333.
- 13 (a) X. Q. Gong, A. Selloni, O. Dulub, P. Jacobson and U. Diebold, *J. Am. Chem. Soc.*, 2008, **130**, 370; (b) Y. Han, C. Liu and Q. Ge, *J. Phys. Chem. C*, 2009, **113**, 20674; (c) Y. Zhou, C. L. Muhich, B. T. Neltner, A. W. Weimer and C. B. Musgrave, *J. Phys. Chem. C*, 2012, **116**, 12114.
- 14 U. Diebold, N. Ruzycski, G. S. Herman and A. Selloni, *Catal. Today*, 2003, **85**, 93.
- 15 (a) A. Furube, T. Asahi, H. Masuhara, H. Yamashita and M. Anpo, *Chem. Phys. Lett.*, 2001, **336**, 424; (b) J. Lee and W. Choi, *J. Phys. Chem. B*, 2005, **109**, 7399.
- 16 K. Peters, *Annu. Rev. Phys. Chem.*, 1987, **38**, 253.
- 17 R. W. Matthews, *J. Chem. Soc., Faraday Trans. 1*, 1989, **85**, 1291.
- 18 S. P. Albu, A. Ghicov, J. M. Macak, R. Hahn and P. Schmuki, *Nano Lett.*, 2007, **7**, 1286.
- 19 C. Pelekani and V. L. Snoeyink, *Carbon*, 2000, **38**, 1423.
- 20 P. W. Atkins, *Physical Chemistry*, Oxford University Press, Oxford, 1986.
- 21 S. M. Mak, B. T. Tey, K. Y. Cheah, W. L. Siew and K. K. Tan, *Adsorption*, 2009, **15**, 507.
- 22 K. Miura, M. Kawase, R. Ashida, I. Gerlach and T. Yamamoto, *Chem. Eng. Sci.*, 2007, **62**, 5655.